

УДК 534.231.2

## СВОЙСТВА СТРУКТУРЫ ПЕРИОДИЧЕСКОГО АКУСТИЧЕСКОГО ИМПЕДАНСА И ВЗАИМОДЕЙСТВИЕ АКУСТИЧЕСКИХ ВОЛН В НОВОМ УПРАВЛЯЕМОМ УСТРОЙСТВЕ НА ПАВ

С.Д. Барсуков<sup>1</sup>, С.А. Хахомов<sup>1</sup>, Д. Кондох<sup>2</sup><sup>1</sup>Гомельский государственный университет им. Ф. Скорины<sup>2</sup>Университет Шизуока, Япония

## FEATURES OF PERIODICAL ACOUSTIC IMPEDANCE STRUCTURE AND ACOUSTIC WAVE INTERACTION IN NOVEL CONTROLLABLE SAW DEVICE

S.D. Barsukou<sup>1</sup>, S.A. Khakhomov<sup>1</sup>, Jun Kondoh<sup>2</sup><sup>1</sup>F. Scorina Gomel State University<sup>2</sup>Shizuoka University, Japan

Приводятся результаты теоретических и экспериментальных исследований устройства на ПАВ с управляемой электроиндуцированной структурой. Принципиально новое устройство на ПАВ было предложено на основе монокристалла LiTaO<sub>3</sub> с объемно-индуцированной управляемой доменной структурой. Параметры индуцированной структуры, а также свойства взаимодействия акустических волн, имеют возможность управления. Изложены теоретические и экспериментальные результаты взаимодействия ПАВ в сегнетоэлектрическом волноводе с различными электроиндуцированными периодическими структурами.

**Ключевые слова:** поверхностные акустические волны (ПАВ), сегнетоэлектрические домены, фононные кристаллы, акустические метаматериалы.

The SAW device with the electroinduced controllable structure was investigated theoretically and experimentally. The innovative SAW device on a LiTaO<sub>3</sub> single crystal with the volume existed and controllable domain structure was proposed. The parameters of the electroinduced structure as well as the acoustic wave interaction have ability to control. The theoretical and experimental results of the acoustic wave interaction in the ferroelectric waveguide with the electroinduced periodical structures were discussed.

**Keywords:** surface acoustic wave (SAW), ferroelectric domain, phonic crystal, acoustic metamaterials.

### Introduction

A surface acoustic wave (SAW) device with novel acoustic metamaterials (AM) and phonic crystal (PCs) structures are increasingly applied in advanced electronics as the broadband filter, negative reflector, signal switcher and so forth [1]–[8]. Current research interest prevails in the ultrasound application area. The perspective effects of ultrasound interaction with PCs and AM structures have been investigated. Recently, the AM structures based on the elementary “metaatoms”, which are characterized by optimal size and shape, opened widespread effects of SAW interaction [9]–[14]. The wave interaction properties are almost determined by the element configuration, size and the array structure [15]–[20]. However, the AMs or 2D analog as the “metasurface” with established parameters and properties do not allow the switching and controlling functionality in real time. Especially, for electronics applications, the controllable interaction of SAW which is the input and output signals are required. In recent years, some studies about the controllable structures have already been discussed [21]–[24]. The controllable electroinduced periodical domain structures on a LiNbO<sub>3</sub> were investigated as a kind of the controllable structures [25]. The switchable

domain structures were induced via the electrostatic effect by applying different electric potentials [26].

In this research the SAW device with an electroinduced controllable structure was theoretically and experimentally studied. The innovative SAW device on a LiTaO<sub>3</sub> single crystal with controllable, electroinduced, and volume existed domain structures was proposed. The periodic domain structures were implemented by the linear electrostatic effect with different electric potentials applied to the surface arranged electrodes. Different electroinduced domain structures are achievable when the electrode structures are crossed on the top and bottom surfaces of the crystal. The parameters of the electroinduced structure and features of the acoustic wave interaction have ability to control. The electroinduced structure is considered as the volume-existed periodic acoustic impedance. The SAW device experimental samples were fabricated, and the propagated SAW influence due to the electroinduced structure was experimentally observed. The theoretical and experimental results of the acoustic wave interaction in ferroelectric waveguide with electroinduced periodical structures were discussed.

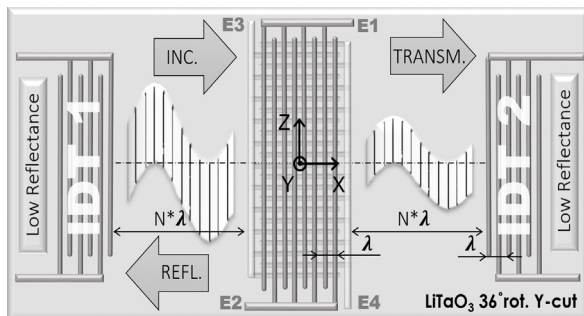
## 1 Principle of the controllable SAW device and theoretical investigations

The SAW device principle and structure are shown in Figure 1.1 (a). The device was fabricated on a  $36^\circ$ -rotated Y-cut, X-propagating  $\text{LiTaO}_3$  single crystal, which allows the shear horizontal (SH) SAW propagation. The SH-SAW propagates as the plate wave with the SH displacements. The resonance frequency and wavelength of the SH-SAW were 10 MHz and  $421 \mu\text{m}$ , respectively. The controlled periodic domain structures were implemented by applying different electric potentials to the surface arranged electrodes of E1, E2, E3, and E4. The electrode fingers arranged on the both surfaces were mutually perpendicular. The applied electric field was lower than the coercive, and the spontaneous domain polarization was not changed. However, the material parameters at the regions of the electric field action are changed. This regime formation of the periodical structure was applied in the current research. Exited from the inter-digital transducer (IDT1) the SH-SAW interacts at the electroinduced structure region, and then the reflected and transmitted waves were generated and registered using the IDT1 and IDT2 simultaneously. At the measurements, the reflected and transmitted SAWs were studied.

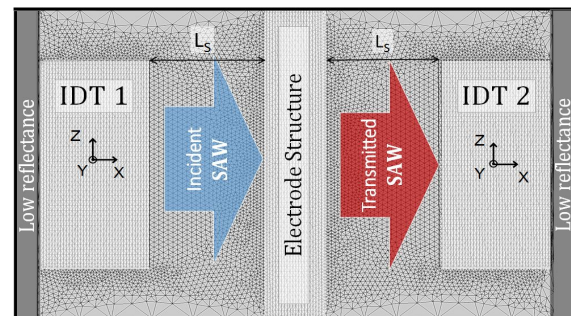
In Ref. [26], the domain formation process for different electrode configurations and ferroelectric substrate thicknesses was discussed. In this research, the finite elements method (FEM) with the full 3D model was applied for the theoretical investigation. The full model of the controllable SAW device was theoretically investigated in two steps in the time domain. The FEM model for the device structure considered is shown in Figure 1.1 (b). In the model the classical descriptions of the electric and relative particle displacements were used. The quasi-static approximation was applied to describe the electric field of the SAW and mechanical stress. All boundaries correspond to the electrical and mechanical potentials absence, and the lateral boundaries

correspond to the low reflection condition. The FEM model includes the IDTs and the electrode structures (ES). The numbers of the electrode fingers of the IDT was 20. The ES consists of 10 electrode fingers on the top and 60 on the bottom surfaces. The distance  $L_S$  between the IDT and ES was 10 wavelengths. The SH-SAW propagated in the X-direction from IDT1 to IDT2. The thickness of the crystal was  $50 \mu\text{m}$ . The total dimension of the calculated structure is  $2000 \times 1000 \times 50 \mu\text{m}^2$ . The electrical potentials of 200 V and 0 V were periodically applied to each pair of the electrode finger of ES. The parameters of the displacements and the electric potential were calculated for the time of  $10 \mu\text{s}$ .

Based on the full model discussed the periodical acoustic impedance structure formation was investigated without the SH-SAW action. This allows discussing the features of formation of induced structure. The results are listed in Figures 1.2 (a) and 1.2 (b). In this model, the domain structure was induced by applying of the opposite DC potentials to the top and bottom ESs simultaneously. When the DC is applied to the ES, the short SH-SAWs are generated and propagated in the opposite form the ES directions. The Figure 1.2 (a) shows the total displacement distribution measured for the time of 1 and  $10 \mu\text{s}$ . The shown displacements correspond to the SAW was induced when the DC is applied. We characterized the periodical structure formation by analyzing spectra of the registered SAW. After the domain structure stabilizes the wave process attenuates. The black curve in Figure 1.2 (b) shows the signal registered by IDT. The short wave packet from 1 to  $3 \mu\text{s}$  corresponds to the domain structure formation signal, and the lower amplitude packet between 4 and  $7 \mu\text{s}$  is the result of the between lateral boundaries and the IDTs reflection. The registered signal spectra are illustrated in Figure 1.2 (b). At least two maximums of 9.6 MHz and 12.8 MHz were observed. The first maximum corresponds to the resonance frequency of the similarity to the IDT structure. The second one relates to the domain



(a)



(b)

Figure 1.1 – (a) Device structure and principle of the SH-SAW interaction; (b) configuration of FEM model of the controllable SAW device (The INC., REFL., and TRANSM. are the incident, reflected, and transmitted waves, respectively. The E1, E2, E3, and E4 are the conductive electrodes arranged on the surface of the acoustic waveguide)

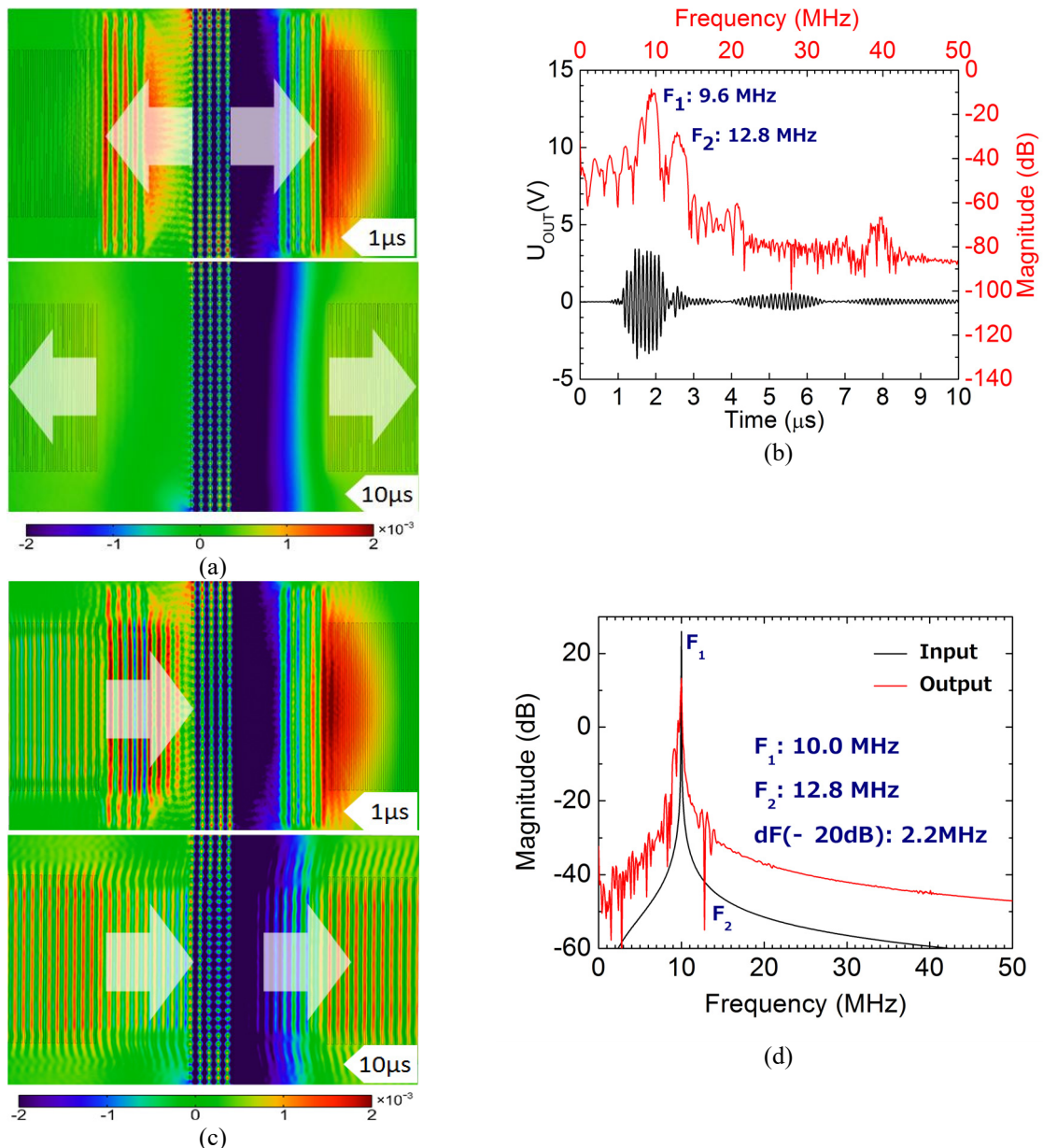


Figure 1.2 – Results of the theoretical investigations: (a) and (b) the periodical structure formation, (c) and (d) the SH-SAW interaction processes. (a) Field of the total displacement distribution measured for the time of 1 and  $10\mu\text{s}$ , (b) the registered of the domain formation signal (the black curve) and spectra (the red curve), (c) the total displacement distribution measured for the time of 1 and  $10\mu\text{s}$  in the case of the SH-SAW interaction, and (d) spectra of the input signal (the red curve) and output signal (the black curve)

formation process, where the displacement was produced in the volume of the crystal.

The acoustic wave interaction includes the SH-SAW transmission, the domain structure formation, and the interaction processes, simultaneously. The SH-SAW interaction was calculated for the time span from 0 to  $10\mu\text{s}$  with results in Figures 1.2 (c) and 1.2 (d). The propagated SH-SAW interacts with the induced periodical structure, and results calculated for the time of 1 and  $10\mu\text{s}$  were plotted in Figure 1.2 (c). Analyzing the displacement distribution in Figure 1.2 (c), the SH-SAW acoustic energy redistribution occurs in the volume of the crystal.

Need to note, that in case of the not matched interaction conditions, the propagation losses will increase. To analyze the acoustic wave interaction, the registered signal spectra (the black curves) and applied signal spectra (the red curve) were compared in Figure 1.2 (d). The resonances of both signals are located at 10 MHz, and related to the SH-SAW propagation. The single minimum of the output signal was found at 12.8 MHz. This result corresponds to the acoustic band gap caused due to SH-SAW interaction with the electroinduced periodical structure.

## 2 Experimental investigations of SAW interaction

Two types of SAW devices with different parameters of the ES were fabricated using a conventional lithography technique. The pitches between the electrode fingers of ES were of 1.0 and 0.5 wavelength. The thickness of the ferroelectric

waveguide was 250  $\mu\text{m}$ . Electrode fingers material for both the IDT and ES was aluminum with thickness about 100 nm. Number of finger pairs for the IDT was 32, and the ES consists of 20 electrode fingers on the top and 116 on the bottom surfaces. The distance between IDT and ES was 32 wavelengths and corresponds to the matched interaction conditions.

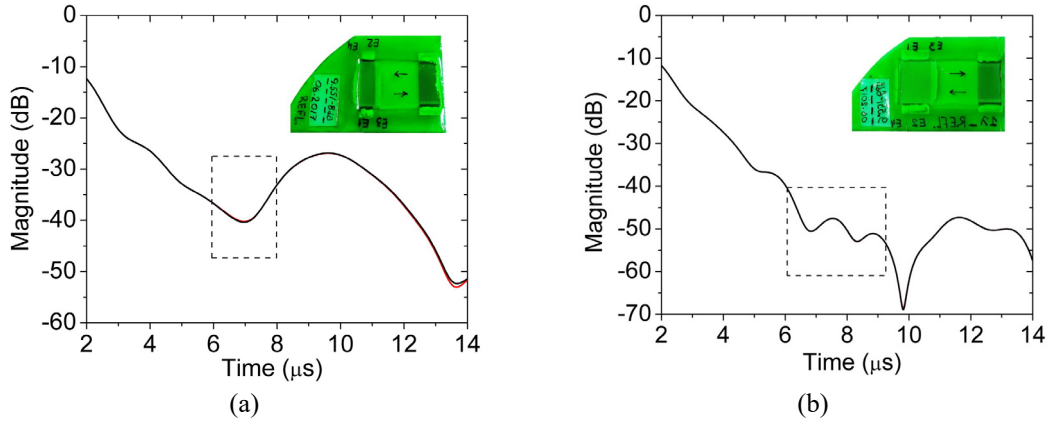


Figure 2.1 – Measured time response and the domain structure region (the dotted curve) and the fabricated sample photograph. (a) The ES with pitch of half wavelength, and (b) the ES with pitch of one wavelength

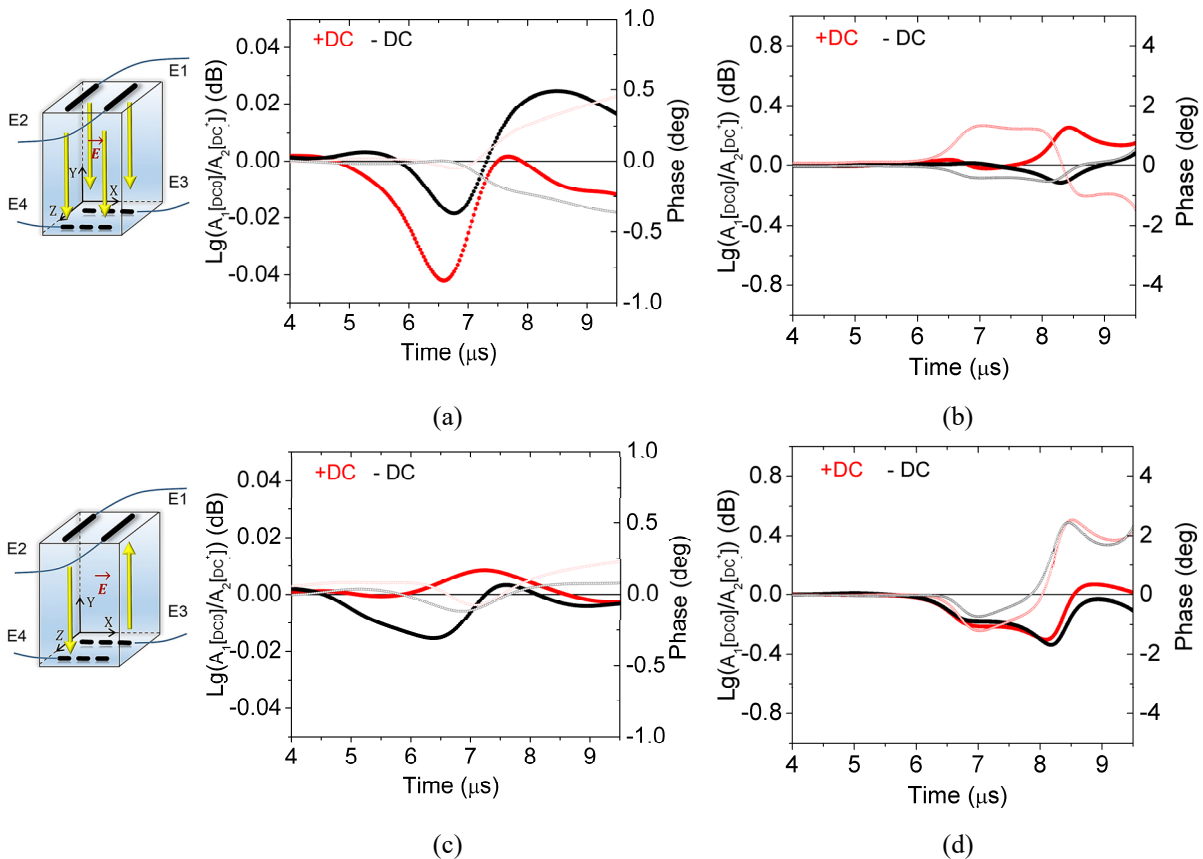


Figure 2.2 – Experimental results of the magnitude relative and phase absolute deviations of the reflected SH-SAW. (a) The domain structure with four codirected domains in the single domain unit and ES pitch of half wavelength, (b) the domain structure with four codirected domains in the domain unit and ES pitch of one wavelength, (c) the domain structure with two opposite directed domains in the domain unit and ES pitch of half wavelength, and (d) the domain structure with two opposite directed domains in the unit and ES pitch of one wavelength

The time response of the reflected signals for the both SH-SAW devices was measured, and the domain induced regions were concluded for both SAW devices. Figures 2.1 (a) and 2.1 (b) shows the measured reflected signals for SH-SAW devices with the pitch of half and one wavelength, respectively. The dashed region shows the location of the induced structure at the timeline scale. Here, the photographs of the fabricated SH-SAW devices with different ES are also shown.

The results of relative magnitude and absolute phase deviation for both studied SAW devices are plotted in Figure 2.2. Here, the results for the periodical structure, which represents the four codirected domains induced in a structural unit, are shown in Figures 2.2 (a) and 2.2 (b). The results obtained for the structure with two opposite directed domains are shown in Figures 2.2 (b) and 2.2 (d). Figures 2.2 (a) and 2.2 (c) describe the results measured for the ES pitch of 0.5, and Figures 2.2 (b) and 2.2 (d) of 1.0 wavelength. The positive +DC (the red curve), and negative –DC (the black curve) polarities of 200 V were applied. The measurement was carried out by the network analyzer (Agilent Technologies, E5070B) in frequency and time domains. To reduce the influence of the “0” level, it was measured for all domain configurations and DC polarities and normalized. During measurements, the ES was “shorted” for AC using the four high voltage capacitance of 0.1 mF connected in “bridge”. That allows reducing the influence occurred during switching of the domain structures. From Figure 2.2 the SH-SAW interaction dependence at the domain induced region on a DC polarity was observed for different domain configurations. Moreover, was found, that the different ESs are provide the different distribution and time shift of the reflected signal. For the ES pitch of one wavelength (Figures 2.2 (b) and 2.2 (d)), the wider region of interaction with different features was observed. However, for the discussed SH-SAW device structure, due to the effects of SH-SAW attenuation and acoustic wave reflection, the matched interaction properties are difficult. The registered signal represents the complex signal from the different acoustic modes which are propagates simultaneously.

In conclusion, the possibilities of the controllable interaction of the SH-SAW with the electroinduced periodical structures were shown theoretically and experimentally. The proposed SAW device structure and discussed interaction features show a good opportunity for advanced electronic applications, such as the controllable filter, delay line, as well as the complex multifunctional device for signal processing. The switchable induced structures allow controlling of the acoustic wave interaction. To achieve the matched conditions of interaction, the SAW device structure improvement is required. The regime of matched interaction allows increasing the SH-SAW parameters and new scattering effects

are reachable. As the way to improve of the domain formation and interaction parameters is the device based on the thin film structure, as well as the appropriate the ferroelectric substrates consideration are required.

#### REFERENCES

1. Hall, D.A. Nonlinearity in piezoelectric ceramics / D.A. Hall // J. Mater. Sci. – 2001. – № 36. – P. 4575.
2. Royer, D. Elastic Waves in Solids I / D. Royer, E. Dieulesain // Springer, Heidelberg. – 2000. – Vol. 1. – P. 216.
3. Microwave a.c. conductivity of domain walls in ferroelectric thin film / A. Tselev, P. Yu, Y. Cao, L.R. Dedon, L.W. Martin, S.V. Kalinin, P. Maksymovych // Nat. Commun. – 2016. – № 7. – P. 11630.
4. Micro- and nano-domain engineering in lithium niobate / V.Y. Shur, E.V. Pelegova, A.R. Akhmatkhanov, I.S. Baturin // Ferroelectrics. – 2016. – № 496:1. – P. 49–69.
5. Whyte, J.R. A diode for ferroelectric domain-wall motion / J.R. Whyte, J.M. Gregg // Nat. Commun. – 2015. – № 6. – P. 7361.
6. Wu, Y. Perspective: Acoustic metamaterials in transition / Y. Wu, M. Yang, P. Sheng // J. Appl. Phys. – 2018. – № 123. – P. 090901.
7. Experimental realization of all-angle negative refraction in acoustic gradient metasurface / B. Liu, B. Ren, J. Zhao, X. Xu, Y. Feng, W. Zhao, Y. Jiang // Appl. Phys. Lett. – 2017. – № 111. – P. 221602.
8. Omnidirectional broadband acoustic absorber based on metamaterials / H. Zhang, B. Liang, X. Zou, J. Yang, J. Yang, J. Cheng // Appl. Phys. Exp. – 2017. – № 10. – P. 027201.
9. Lithium niobate phononic crystals for tailoring performance of RF laterally vibrating devices / R. Lu, T. Manzanecque, Y. Yang, S. Gong // IEEE Trans. – 2018. – № 65 (6). – P. 934–944.
10. Measurement of a broadband negative index with space-coiling acoustic metamaterials / Y. Xie, B. Popa, L. Zigoneanu, S.A. Cummer // Phys. Rev. Lett. – 2013. – № 110. – P. 175501.
11. Design of an acoustic metamaterial lens using genetic algorithms / D. Li, L. Zigoneanu, B. Popa, S.A. Cummer // J. Acoust. Soc. Am. – 2012. – № 132. – P. 2823.
12. Zigoneanu, L. Design and measurements of a broadband two-dimensional acoustic lens / L. Zigoneanu, B. Popa, S.A. Cummer // Phys. Rev. B. – 2011. – № 84. – P. 024305.
13. Three-dimensional labyrinthine acoustic metamaterials / T. Frenzel, J. D. Brehm, T. Buckmann, R. Schittny, M. Kadic, M. Wegener // Appl. Phys. Lett. – 2013. – № 103. – P. 061907.
14. High-Q micromechanical resonators in a two-dimensional phononic crystal slab / S. Mohammadi, A.A. Eftekhar, W.D. Hunt, A. Adibi // Appl. Phys. Lett. – 2009. – № 94. – P. 01KB05.

15. *Iwasaki, Y.* Rectification of Lamb wave propagation in thin plates with piezo-dielectric periodic structures / Y. Iwasaki, K. Tsuruta, A. Ishikawa // *Jpn. J. Appl. Phys.* – 2016. – № 55. – P. 07KB02.
16. *Liang, B.* Acoustic diode: rectification of acoustic energy flux in one-dimensional systems / B. Liang, B. Yuan, J. Cheng // *Phys. Rev. Lett.* – 2009. – № 103. – P. 104301.
17. *Lu, M.* Phononic crystals and acoustic metamaterials / M. Lu, L. Feng, Y. Chen // *J. Materials Today.* – 2009. – № 12 (12). – P. 34–42.
18. *Laude, V.* Stochastic excitation method for calculating the resolvent band structure of periodic media and waveguides / V. Laude, M.E. Korotyaeva // *Phys. Rev. B.* – 2018. – № 97. – P. 224110.
19. *Acoustic far-field focusing effect for two-dimensional graded negative refractive-index sonic crystals* / S. Peng, Z. He, H. Jia, A. Zhang, C. Qiu, M. Ke, Z. Liu // *Appl. Phys. Lett.* – 2010. – № 96. – P. 263502.
20. *Electrical tuning of dc bias induced acoustic resonances in paraelectric thin films* / A. Noeth, T. Yamada, A.K. Tagantsev, N. Setter // *J. Appl. Phys.* – 2008. – № 104. – P. 094102.
21. *Active acoustic metamaterials reconfigurable in real time* / A. Popa, D. Shinde, A. Konneker, S.A. Cummer // *Phys. Rev. B.* – 2015. – № 91. – P. 220303.
22. *Chen, Z.* Tunable topological phononic crystals / Z. Chen, Y. Wu // *Phys. Rev. Appl.* – 2016. – № 5. – P. 054021.
23. *Pashchenko, V.P.* Controlled surface acoustic wave phononic crystal based on induced periodic domains / V.P. Pashchenko // *Proc. St. Petersburg State Polytechnic University.* – 2013. – № 3 (177). – P. 55–59.
24. *Barsukov, S.D.* Acoustic waves in ceramics with the electroinduced anisotropy / S.D. Barsukov, S.A. Khakhomov, I.V. Semchenko // *Journal of Automation, Mobile Robotics and Intelligent Systems.* – 2009. – Vol. 3, № 4. – P. 34.
25. *Periodic domain inversion in x-cut single-crystal lithium niobate thin film* / P. Mackwitz, M. Rüsing, G. Berth, A. Widhalm, K.Müller, A. Zrenner // *Appl. Phys. Lett.* – 2016. – № 108. – P. 152902.
26. *Barsukov, S.D.* Investigation of interaction of shear horizontal surface acoustic wave with controlled electroinduced domain structure / S.D. Barsukov, J. Kondoh // *Jpn. J. Appl. Phys.* – 2017. – № 56. – P. 07JD07.

Поступила в редакцию 21.09.18.